International Journal of Chronic Obstructive Pulmonary Disease

Dovepress
Taylor & Francis Group

Open Access Full Text Article

ORIGINAL RESEARCH

PulmoClass-3DAtt: A Self-Attention Network for Classification of COPD, PRISm and Normal

Qian Wu, Ruihan Li, Hui Guo, Jinhuan Han, Zhen Zhang, Ayajiang Jingesi, ShuQin Kang

Department of Medical Imaging Center, The Fourth Clinical Medical College of Xinjiang Medical University, Urumqi, Xinjiang, People's Republic of China

Correspondence: Hui Guo, Department of Medical Imaging Center, The Fourth Clinical Medical College of Xinjiang Medical University, Urumqi, Xinjiang, 830000, People's Republic of China, Email guohui9804@126.com

Background: Chronic obstructive pulmonary disease (COPD) is the third leading cause of death worldwide, making its accurate diagnosis critical. It is difficult to distinguish COPD from preserved ratio impaired spirometry (PRISm), due to their shared small-airway pathology. This study develops a novel deep-learning framework that combines chest CT images with clinical variables to discriminate between COPD, PRISm, and normal categories.

Methods: In this retrospective study, consecutive subjects were enrolled from a university-affiliated tertiary hospital between January 2018 and June 2024. After random split at an 8:2 ratio, the training cohort was used to develop a convolutional encoder that extracts imaging features and simultaneously predicts five spirometric parameters (FEV_1, FVC, FEV_1/FVC, FEV_1 %pred, FVC %pred). The extracted features were then fed into the self-attention deep-learning model PulmoClass-3DAtt, which was trained and fine-tuned through ten-fold cross-validation to classify disease status. Classification performance was quantified by the area under the receiver-operating-characteristic curve (AUC), overall accuracy (ACC), precision (Pre), sensitivity (Se) and specificity (Sp). Regression performance for spirometric indices was assessed with mean-squared error (MSE), mean absolute error (MAE) and concordance correlation coefficient (CCC).

Results: The cohort comprised 1918 participants (1362 COPD, 174 PRISm, 382 normal controls). The model achieved robust overall performance (AUC = 0.86, ACC = 0.87). For COPD, Normal and PRISm the respective values are ACC 0.87, 0.88, 0.87; Se 0.90, 0.88, 0.42; Sp 0.84, 0.88, 0.97; Pre 0.85, 0.79, 0.72; and F1-score 0.88, 0.85, 0.53. In the validation set, the five spirometric metrics were predicted with MSE 0.03–0.35, MAE 0.14–0.46 and CCC 0.56–0.83.

Conclusion: By integrating multimodal imaging–function data through a self-attention framework, PulmoClass-3DAtt reliably discriminates among COPD, PRISm and normal status, providing an immediately applicable tool for clinical decision support and the delivery of precision pulmonary medicine.

Plain Language Summary:

(1) This study furnishes the first feasibility evidence that a self-attention deep-learning architecture can discriminate among chronic respiratory diseases, establishing a reusable paradigm for future investigations while directly informing clinical decision-making and disease stewardship.
(2) By supplying an image-based, equipment-agnostic classifier, the model offers a globally deployable, low-cost solution to the widespread under-diagnosis and misclassification of lung-function impairment.
(3) Simultaneous prediction of spirometric indices from routine CT and readily available clinical data enables real-time grading of disease severity and individualised planning of follow-up therapy without additional patient burden.

Keywords: chronic obstructive pulmonary disease, preserved ratio impaired spirometry, deep learning, self-attention, transformer, chest CT

Introduction

Chronic respiratory diseases have ranked as the third leading cause of death worldwide since 2010, imposing a substantial burden on global health. Among these disorders, chronic obstructive pulmonary disease (COPD) is the most prevalent and clinically significant. The etiology of COPD encompasses genetic susceptibility, environmental exposures, and respiratory

https://doi.org/10.2147/COPD.S573618
Received: 24 October 2025
Accepted: 13 February 2026
Published: 26 February 2026

infections; however, long-term cigarette smoking remains the predominant and most critical risk factor. Population ageing is expected to further increase the economic strain on COPD patients. In 2019, annual medical expenditures for COPD in the United States reached $31.3 billion and are projected to rise to $60.5 billion by 2029.[1] A large Canadian population-based study reported that COPD patients incurred 48% higher excess healthcare costs than individuals without COPD.[2] China, bearing the world's greatest absolute economic burden of COPD, accounts for 83.5% of disease-related economic losses among middle- and high-income countries.[3] Early screening and identification of COPD can therefore prevent disease progression and mitigate both health and economic burdens.

Twenty years ago, researchers observed that some patients presented with respiratory symptoms and imaging abnormalities yet did not fulfil traditional spirometric criteria for COPD. A decade later, the Global Initiative for Chronic Obstructive Lung Disease (GOLD) was the first to designate this phenotype "preserved ratio impaired spirometry" (PRISm) and initiated systematic investigation. Across multiple cohorts, PRISm prevalence has ranged from 4.49 to 24.4%,[4–6] variations attributable to population characteristics and regional differences. The PRISm phenotype is inherently unstable.[7] Established risk factors for progression to COPD include advanced age, male sex, abnormal body-mass index, and heavy smoking.[8,9] Formal recognition arrived only with the 2023 Global Initiative for Chronic Obstructive Lung Disease, which defined PRISm as a potential pre-COPD state and called for heightened clinical vigilance.[10] PRISm is now recognised as an independent risk factor for incident COPD.[11,12]

However, in real-world clinical practice, approximately one-quarter of patients already diagnosed with—and receiving treatment for—COPD do not fulfil the spirometric criteria recommended by GOLD and instead meet definitions of pre-COPD or PRISm.[13,14] Diagnosis of PRISm relies primarily on spirometry; ancillary assessments include chest CT, pulse oximetry,[15] and selected biomarkers.[16,17] PRISm is defined as a post-bronchodilator $FEV_1/FVC \geq 0.7$ with FEV_1 (or FVC) < 80% of the predicted value.

Pulmonary function test (PFT) remains the gold standard for diagnosing both COPD and PRISm; however, their accuracy depends on high patient cooperation, and under- or misdiagnosis remains common.[18] In primary-care settings, PFT is still underutilised, resulting in delayed or missed diagnoses.[19] Chest CT, which offers the most direct structural information about lung pathology, has emerged as an alternative.[20,21] Yet visual assessment of large CT datasets is inherently subjective and labour-intensive, particularly in individuals with impaired lung function, such as COPD and PRISm patients. Over the past decade, artificial intelligence (AI) has become deeply integrated into healthcare,[22–24] and deep learning—by automatically extracting features from high-dimensional data—has gained prominence in the last two years. These models substantially enhance disease management and reduce clinical workload, achieving notable advances in the diagnosis, staging, prediction, and prognostication of thoracic disease.[25–27]

On CT imaging, COPD is defined by the dual signature of emphysematous destruction and/or small-airway disease, whereas PRISm is pathophysiologically heterogeneous: beyond subtle parenchymal changes, obesity, chest-wall deformities or metabolic insults can constitute the primary driver. These disparate mechanisms produce overlapping early phenotypes that are virtually indistinguishable on visual inspection, yet they mandate divergent therapeutic trajectories—symptom-oriented bronchodilation and anti-inflammatory regimens for COPD versus cause-targeted intervention (weight reduction, metabolic optimisation or surgical correction) for PRISm. Consequently, a rapid, image-based discriminator is a critical lever for evidence-based, disease-specific management.

To the best of our knowledge, no prior study has leveraged CT imaging to develop a deep-learning discriminator between COPD and PRISm; existing work is confined to traditional radiological scoring or conventional machine-learning algorithms. To bridge this gap, we introduce PulmoClass-3DAtt, the first self-attention-driven model that fuses three-dimensional CT morphological signatures with routinely available clinical variables to simultaneously classify disease and quantify severity. By concurrently predicting five canonical spirometric indices, the system furnishes clinicians with an immediate, objective proxy of functional impairment, thereby guiding phenotype-specific therapy and longitudinal management.

Research Review

A summary of studies that have employed AI models for the diagnosis and classification of PRISm is presented in Table 1.

Table 1 Summary of AI-Based Investigations into PRISm Diagnosis and Classification

Study	Model	Year	Country	Sample Size	Data	Results and Classes
Zhou et al[28]	Radiomics	2024	China	1481	CT images	PRISm and normal (AUC: 0.79; SE: 0.75; SP: 0.69)
Zhou et al[29]	Radiomics	2024	China	1066	CT images	PRISm and COPD (AUC: 0.84; ACC: 0.73; SE: 0.90; SP: 0.56)
Lukhumaidze et al[30]	Machine learning+ radiomics	2025	Canada	596 (CanCOLD)	CT images	Stable PRISm and stable control (AUC: 0.84, Recall: 0.92, F1 score: 0.54) Stable PRISm and stable COPD (AUC: 0.92, Recall: 0.87, F1 score: 0.60)
Ratiu et al[31]	Machine learning	2025	China	367	Volatile organic compounds	PRISm and healthy control (AUC: 0.78, SP: 0.69, SE: 0.87) PRISm and asthma (AUC: 0.74, SP: 0.82, SE: 0.66)

Abbreviation: CanCOLD, A public dataset from Canada.

Materials and Methods

Our Institutional Review Board approved this retrospective study and waived the requirement for informed written consent (2025XE0165).

Participants and Dataset

We retrospectively enrolled consecutive patients who underwent both PFT and chest CT at the Fourth Clinical Medical College of Xinjiang Medical University between January 2018 and June 2024. Owing to the retrospective design, informed consent was waived. Medical records were reviewed for baseline clinical data and thin-section CT images. Inclusion criteria: (1) interval between CT and PFT $\leq$ 1 month; (2) complete thin-section CT acquisition. Exclusion criteria: (1) coexisting thoracic disorders (eg, extensive atelectasis, pneumonia); (2) suboptimal image quality or artefacts. Ultimately, 1918 participants were analysed. 1164 subjects were randomly selected and further subdivided into an 8:2 training-to-validation ratio for encoder development, while the remaining 754 subjects, kept fully independent, were used to construct and internally validate the PulmoClass-3DAtt classifier through rigorous ten-fold cross-validation. The complete dataset-curation workflow is illustrated in Figure 1.

The patients received detailed instructions and repeated breath-holding training to ensure maximum deep inspiration during the chest CT scan. CT examinations were performed on Siemens and GE Healthcare scanners. Whole-chest axial images were acquired at full inspiration using 120 kV, 1.25 mm slice thickness; tube current, exposure time, and in-plane pixel size were patient-specific. Spirometric classification followed GOLD guidelines: normal—post-bronchodilator $FEV_1/FVC \geq 0.7$ and FEV_1 (or FVC) $\geq$ 80% predicted; PRISm—$FEV_1/FVC \geq 0.7$ and FEV_1 (or FVC) < 80% predicted; COPD—$FEV_1/FVC < 0.7$. See Table S1 of supplementary material for details.

Data Preprocessing

To mitigate vendor- and protocol-related heterogeneity, CT volumes were clipped to a unified window (−1000 to +600 HU), resampled to 128×128×128 voxels via trilinear interpolation and z-score normalised. Lung parenchyma was automatically segmented with the open-source U-Net (R231) model (https://github.com/JoHof/lungmask), previously validated on multiple large-scale datasets. Two thoracic radiologists (Guo H, 10 years; Kang SQ, 5 years) independently segmented 50 randomly selected cases using 3D Slicer v4.10 (https://www.slicer.org) to verify the algorithm; the resulting masks were reviewed and confirmed by two additional radiologists (Wu Q, Li RH). To ensure anonymity, Zhang Z and Jingesi A assigned a random, mismatched, unique identifier to every scan without participating in segmentation or interpretation. Dice coefficients for Guo H and Kang SQ were 0.96 and 0.94, respectively, with an inter-reader ICC of 0.96. The complete deep-learning model workflow is summarised in Figure 2.

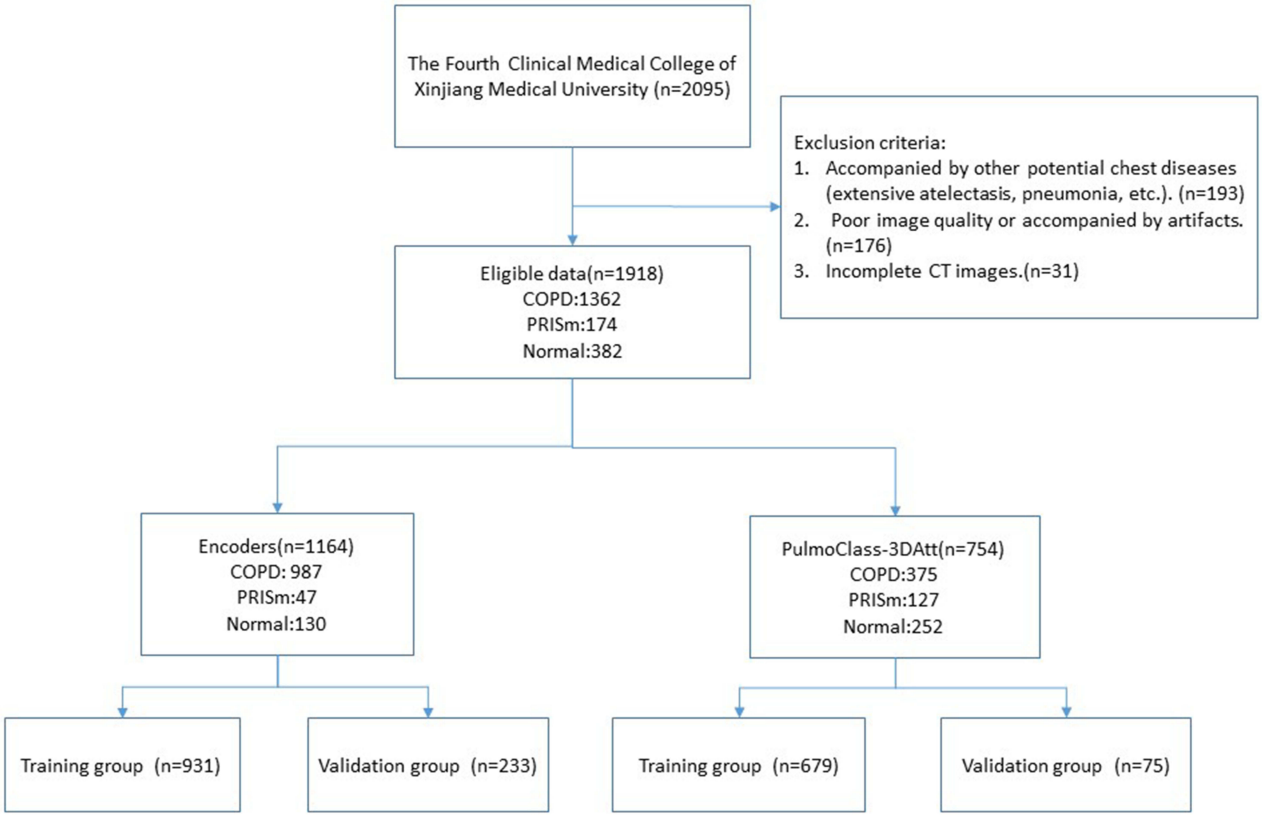

Figure 1 Dataset-curation workflow.

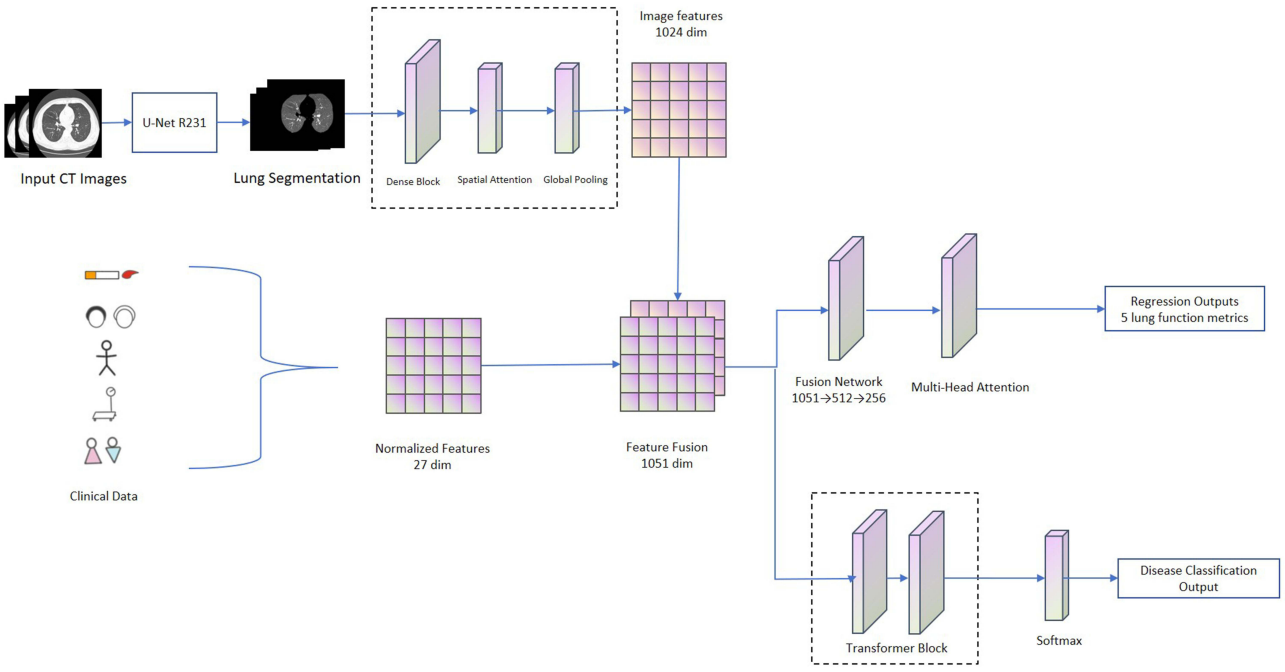

Figure 2 Deep-learning model workflow.

Deep Learning Model Development

Encoder

The feature encoder is built upon a 3D DenseNet-121 backbone that achieves incremental, multi-scale fusion through its hallmark dense-connectivity paradigm. An initial 7×7×7 convolutional layer captures low-level anatomical signatures with stride 2, followed by four successive dense blocks that progressively deepen feature abstraction. Within each block, multiple 3D convolutional units—standardised as batch-normalisation → ReLU → 3×3×3 convolution—are concatenated with all preceding feature maps via the reuse pathway, guaranteeing maximum gradient flow and parameter efficiency while preserving high-resolution parenchymal detail.

Following the last dense block, we embed a novel 3D spatial-attention module: a 1×1×1 convolution first squeezes the channel axis, and a subsequent Sigmoid gating produces voxel-level importance weights that adaptively amplify voxels harboring pathology. Global-average-pooling then collapses the 3D feature space into a 1024-dimensional descriptor. This design preserves spatial integrity while heightening sensitivity to key alterations—emphysematous foci, bronchial-wall thickening—and dynamically up-weights small-airway regions critical to PRISm. The resulting imaging signature is concatenated with available clinical variables and forwarded to PulmoClass-3DAtt, where ten-fold cross-validation performs disease classification.

Self-Attention Classifier System (PulmoClass-3DAtt)

The PulmoClass-3DAtt classifier is built on a Transformer encoder that models global feature interactions via a multi-head self-attention mechanism. First, the 1024-dimensional image–clinical fused descriptor is linearly projected into a 128-dimensional semantic space; learnable 3D positional encodings are added to preserve spatial relationships. The core is an eight-head parallel attention layer: each head independently computes scaled dot-product attention weights between every feature vector, yielding a context-aware representation that emphasises pathology-bearing voxels. Two successive Transformer blocks—each comprising residual-connected, layer-normalised multi-head attention followed by a 2-layer feed-forward network with GELU activation—further integrate long-range dependencies and supply non-linear transform capacity. This design allows the model to automatically focus on the anatomical micro-territories critical to PRISm and to boost detection sensitivity for spatially discrete lesions.

Statistical Analysis

Statistical analysis was performed with IBM SPSS Statistics 27. Continuous variables are presented as mean ± SD, and categorical variables as counts and proportions. Inter-group differences among controls, PRISm and COPD subjects were assessed by one-way ANOVA for continuous variables and the χ^2-test for categorical variables; statistical significance was set at $p < 0.05$.

All deep-learning evaluations were conducted in Python 3.10. To counteract the small PRISm sample, a stratified 10-fold cross-validation scheme was employed. ROC curves and confusion matrices were generated to derive ACC, AUC, sensitivity (Se), specificity (Sp) and F1-score. Pulmonary-function prediction was assessed with the mean squared error (MSE), mean absolute error (MAE), and concordance correlation coefficient (CCC). Gradient-weighted class activation mapping (Grad-CAM) was applied to produce voxel-level heat maps for model interpretation.

Results

Baseline Characteristics of Participants

Table 2 summarises the demographic, clinical and spirometric profile of the 1918 enrolled subjects. Overall, 1362 (71.0%) had COPD, 382 (19.9%) were normal controls and 174 (9.1%) met PRISm criteria. Mean age was 66 ± 11 years; 1271 participants (66.3%) were male and 647 (33.7%) female. Average height and weight were 165.1 ± 8.2 cm and 68.3 ± 11.9 kg, respectively. Smoking history was distributed as never-smokers n = 1070, ex-smokers n = 429 and current smokers n = 419. Spirometric means were: FEV_1 1.7 ± 0.8 L, FVC 2.7 ± 0.9 L, FEV_1/FVC 0.60 ± 0.10, FEV_1 %pred 0.70 ± 0.30 and FVC %pred 0.80 ± 0.20. Among the COPD group, the smoking rate was 47.4% (645/1362), exceeding that of the PRISm (40.2%) and Normal (34.8%) groups.

Table 2 Baseline Characteristics of Participants

Characteristic	Mean (±std)/Count (Proportion %)
Man/Female, n (%)	1271/647 (66.3%/33.7%)
Age, year	66±11
Height, cm	165.1±8.2
Weight, kg	68.3±11.9
Never/Former/Current Smokers, n (%)	1070/429/419 (55.8%/22.4%/21.8%)
FEV_1 (L)	1.7±0.8
FVC (L)	2.7±0.9
FEV_1/FVC	0.6±0.1
FEV_1 %pred	0.7±0.3
FVC %pred	0.8±0.2
COPD/Normal/PRISm	1362/382/174 (71.0%/19.9%/9.1%)

Abbreviations: FEV_1, 1-s forced expiratory volume; FVC, forced vital capacity; FEV_1/FVC, 1-s forced expiratory volume ratio forced vital capacity; FEV_1 %pred, 1-s forced expiratory volume to predicted value; FVC %pred, forced vital capacity to predicted value.

The encoder cohort comprised 1164 subjects: 11.2% Normal, 4.0% PRISm and 84.8% COPD. The deep-learning model cohort comprised 754 subjects: 33.4% Normal, 16.8% PRISm and 49.7% COPD. All five pulmonary function indices differed significantly across the three groups. Post-hoc analyses revealed no significant difference in FVC or FVC %pred between COPD and PRISm, nor in FEV_1/FVC between PRISm and Normal. All other pairwise comparisons were significant. See Tables S2 and S3 of Supplementary Materials for details.

Classification Performance of Deep Learning Model Based on Self-Attention Mechanism

Table 3 summarises the performance metrics of the PulmoClass-3DAtt mo the corresponding confusion matrix and ROC curves are displayed in Figures 3 and 4 respectively. Sensitivity and specificity curves of the overall classification of the model are displayed in Figure 5. The self-attention deep-learning model PulmoClass-3DAtt achieved an overall three-class AUC of 0.86. For COPD it delivered high and balanced performance with Se 0.90, Sp 0.84, Pre 0.85 and F1-score 0.88, permitting accurate detection while rarely assigning the label to non-COPD cases. Normal subjects were identified with similarly robust Se (0.88) and Sp (0.88), although Pre was slightly lower (0.79) because a few COPD or PRISm individuals were occasionally predicted as normal—an error rate deemed clinically acceptable For PRISm, the high SP (0.97) and ACC (0.87) indicate that the model rarely mislabels either COPD or healthy subjects as PRISm, underscoring the need to refer screen-positive individuals for confirmatory spirometry. Yet the low Se (0.42) implies a meaningful rate of missed PRISm diagnoses.

Typical COPD is characterized by persistent airflow limitation, with imaging features such as emphysema and airway wall thickening that are prominent, objective, and easily captured by the model. In contrast, PRISm is highly heterogeneous, with diverse causes including small airway disease, early interstitial lung disease, thoracic deformity, and obesity, leading to variable imaging manifestations. In cases of small airway related PRISm, CT findings may only show air trapping, which is subtle and easily overlooked. For PRISm caused by non pulmonary factors, lung CT may appear

Table 3 The Performance Metrics of PulmoClass-3DAtt

	Sensitivity	Specificity	Precision	F1-score	ACC	AUC
COPD	0.90	0.84	0.85	0.88	0.87	0.86
Normal	0.88	0.88	0.79	0.83	0.88	
PRISm	0.42	0.97	0.72	0.53	0.87	

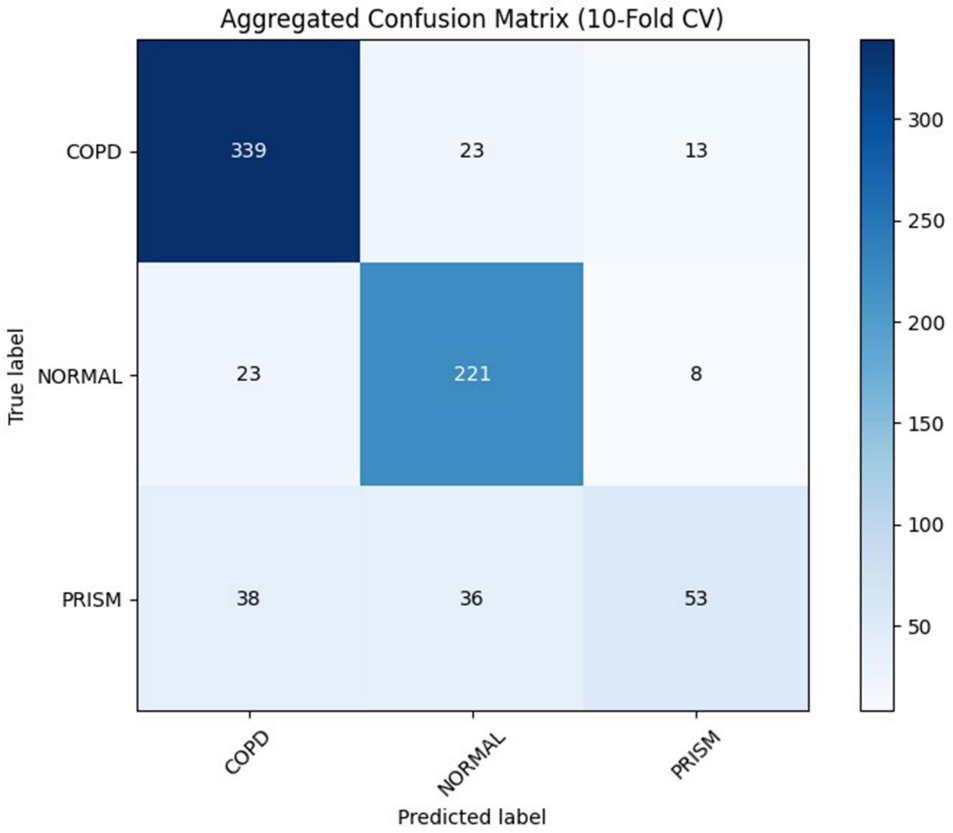

Figure 3 The confusion matrix of the PulmoClass-3DAtt model.

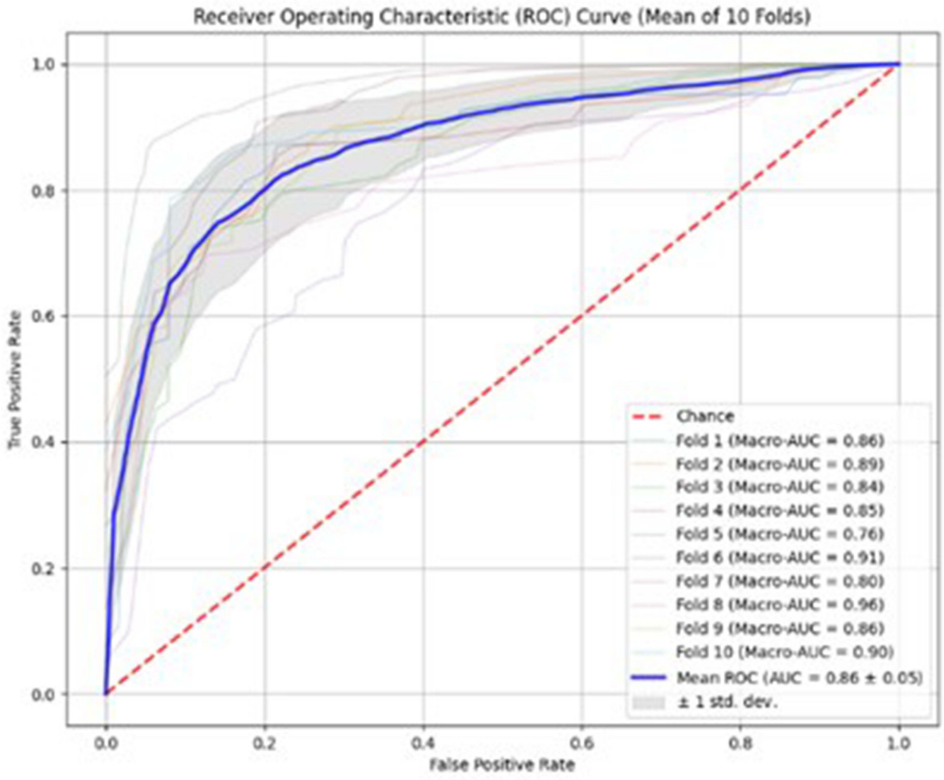

Figure 4 The receiver operating characteristic curves of the PulmoClass-3DAtt model.

https://doi.org/10.2147/COPD.S573618

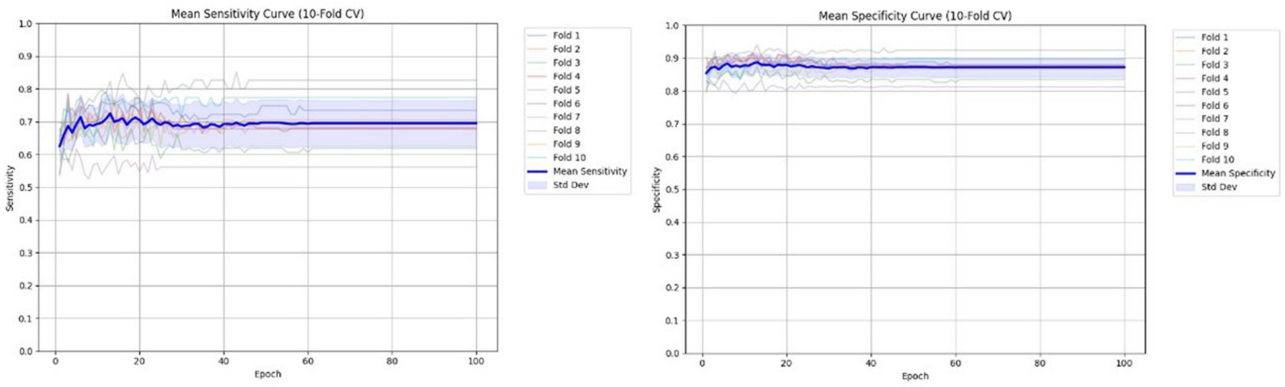

Figure 5 Sensitivity and specificity curves of the overall classification of the PulmoClass-3DAtt model (sensitivity on the left and specificity on the right). The two curves tend to be stable in the early training period (about 20 epoch).

completely normal or show only slight compressive atelectasis, highly overlapping with normal imaging. This explains the low Se in PRISm classification.

Evaluation of Predictive Performance of Lung Function Index of Encoder

Table 4 summarises the encoder's predictive performance for the five spirometric variables. In the training set MSE ranged from 0.01 to 0.14, MAE from 0.09 to 0.29 and CCC from 0.81 to 0.92, indicating close agreement with the reference measurements. Performance declined in the validation set, where MSE was 0.03–0.35, MAE 0.14–0.46 and CCC 0.56–0.83; the largest drop was observed for FVC %pred. Among the five indices, FVC itself was predicted most accurately, whereas FEV_1 %pred and, more markedly, FVC %pred showed the poorest agreement. Clinically, this limitation probably reflects the omission of diaphragmatic and mediastinal information from the segmented CT volume, compounded by the double uncertainty arising from population-based prediction equations that do not capture individual anthropometric variation.

The model successfully links imaging structure with pulmonary function, validating its potential to reveal the intrinsic pathophysiology of disease. FEV_1, FVC, and their ratio directly reflect lung geometry, and CT clearly depicts lobar volume loss, emphysematous destruction, small airway narrowing, and interstitial distortion such as fibrosis. By encoding these whole lung morphological signatures, the system enables rapid, objective grading of COPD severity and fibrotic burden. In contrast, FEV_1 predicted and FVC predicted incorporate complex individual factors, explaining their lower personalized prediction accuracy.

Feature Extraction Visualization

Grad-CAM extracts visual heat map features and addresses the lack of transparency in AI models. Bright regions indicate high model attention weights, meaning these areas significantly contribute to the current category prediction, while dark regions indicate low attention weights and minimal contribution to the prediction. As shown in Figure 6, the axial bitmap

Table 4 Encoder Lung Function Prediction Performance

	Training Set (n=931)					Validation Set (n=233)				
	MSE	**MAE**	**CCC**	**R**	**R2**	**MSE**	**MAE**	**CCC**	**R**	**R2**
FEV_1	0.14	0.29	0.89	0.90	0.81	0.35	0.46	0.77	0.81	0.64
FVC	0.08	0.22	0.92	0.93	0.86	0.22	0.35	0.83	0.85	0.72
FEV_1/FVC	0.01	0.06	0.85	0.86	0.73	0.01	0.07	0.78	0.80	0.62
FEV_1 %pred	0.01	0.09	0.89	0.89	0.80	0.04	0.14	0.72	0.76	0.58
FVC %pred	0.01	0.09	0.81	0.83	0.69	0.03	0.14	0.56	0.64	0.41

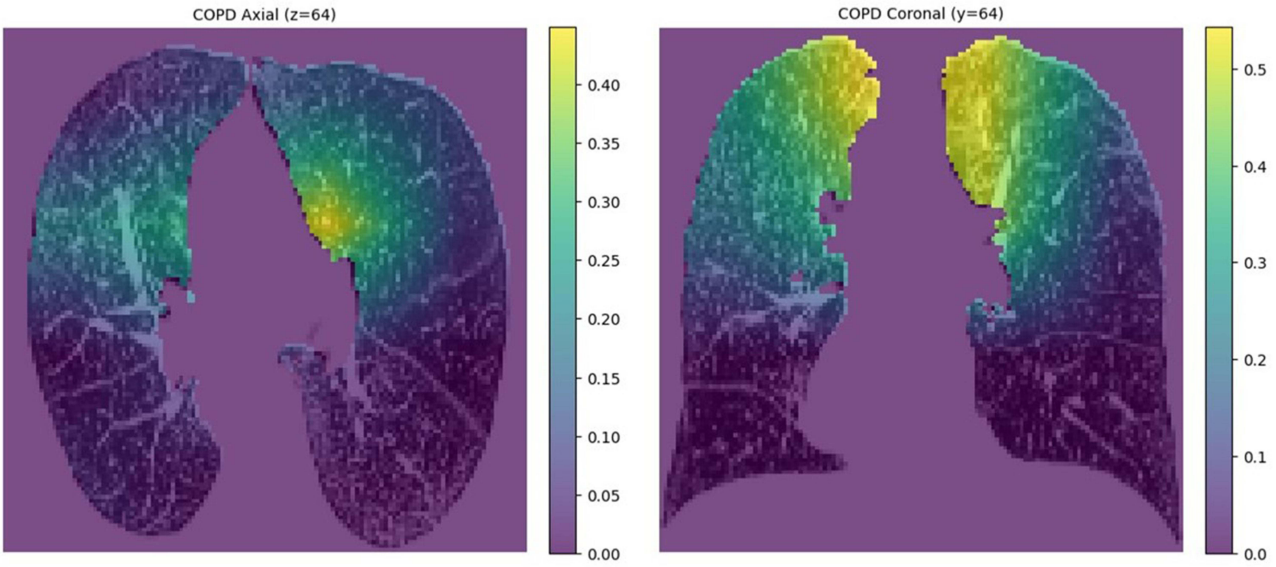

Figure 6 Visualisation heat map of feature extraction. The patient is a 60-year-old man with COPD (FEV_1 0.66 L, FVC 2.13 L, FEV_1/FVC 0.31, FEV_1 %pred 0.25, FVC %pred 0.62).

displays highlighted areas mainly around the bronchi, while the coronal bitmap shows highlighted areas primarily concentrated at the lung apex. This distribution pattern aligns with the typical upper lobe emphysema distribution observed in COPD patients.

Discussion

COPD is common and imposes a heavy burden, yet spirometric screening rates remain low, leaving many cases undetected. Consequently, alternative diagnostic modalities are gaining importance. The widespread use of chest CT now allows functional inferences from structural lung data, and continuous AI model refinement has further improved both efficiency and accuracy.[32–34] Our model enables early identification of high-risk individuals, facilitating prompt intervention. Advanced age, male sex, abnormal BMI, and heavy smoking are well-established drivers of PRISm-to-COPD progression, and elevated inflammatory markers have also been implicated.[35,36] We therefore incorporated age, sex, height, weight, and smoking status as clinical baseline variables together with CT imaging features for disease classification. While AI-based COPD diagnostics have been extensively studied,[37–39] investigations using AI to identify and classify PRISm on CT images remain scarce.

Zhou et al[28,29] constructed a CT-based radiomics model to distinguish PRISm from COPD and improved its performance by integrating clinical variables. Lukhumaidze et al[30] developed three CT-driven machine-learning models—logistic regression, random forest, and support vector machines—for pairwise classification of stable PRISm, stable controls, and stable COPD, identifying discriminative features in the process. Our study transcends the constraints of conventional binary classification by introducing the first deep-learning framework that simultaneously discriminates COPD, PRISm, and normal individuals—an approach that more closely aligns with clinical demands. Moreover, an end-to-end encoder automatically learns deep imaging features without reliance on hand-crafted radiomics, while an innovative multi-task pipeline jointly optimises lung-function prediction and three-class classification, yielding higher-precision screening. AI innovation and interdisciplinary collaboration not only enhance disease management but also support junior clinicians, relieve diagnostic pressure on hospitals, and narrow regional healthcare disparities.[40,41] Future work can extend this paradigm to chest X-ray and MRI.[42–45]

Accurate discrimination among COPD, PRISm and normal is essential for patient-centred disease management. Here we developed and externally validated an end-to-end deep-learning pipeline that performs fully automated three-class classification on volumetric chest CT. A depth encoder first fuses high-resolution CT with paired clinical variables; the resultant representation is fed into PulmoClass-3DAtt, a 3D self-attention network. On the validation set, the five

spirometric indices were predicted with MSE 0.03–0.35, MAE 0.14–0.46 and CCC 0.56–0.83; FVC yielded the best agreement, and FVC %-predicted the lowest. In the disease-classification task, the model achieved robust overall performance (AUC = 0.86, ACC = 0.87). For COPD, Normal and PRISm the respective values are ACC 0.87, 0.88, 0.87; Se 0.90, 0.88, 0.42; Sp 0.84, 0.88, 0.97; Pre 0.85, 0.79, 0.72; and F1-score 0.88, 0.85, 0.53. COPD and Normal categories achieved strong classification metrics, whereas PRISm showed the lowest Se (0.42), implying a high false-negative rate that likely stems from its often subtle or atypical imaging features; this under-detection will be a focal point for future work. Nevertheless, PRISm attained the highest Sp (0.97), translating to a low false-positive rate and underscoring the value of referring screen-positive individuals for definitive spirometry. Looking ahead, an AI-driven two-class model that separates either COPD or PRISm from Normal could offer a practical tool for flagging patients with overt disease or latent risk. As recognition and diagnostic criteria for Pre-COPD sharpen, this stage will emerge as a promising research focus, enabling population-wide risk screening.

This study benefits from a sufficiently large sample of 1918 participants, enhancing the model's generalisability. Whereas prior work was forced into binary classification by limited data, we present the first CT-based deep-learning system that discriminates among COPD, PRISm and normal, aligning the algorithm with real-world clinical encounters. By additionally harnessing multimodal imaging–clinical features to predict five spirometric indices, we furnish simultaneous categorical and quantitative estimates of disease severity, an advance that streamlines triage and informs individualised management. The framework therefore offers clinicians a faster, non-invasive and reproducible tool, holds promise for slowing progression, lessening patient burden and accelerating the transition to precision respiratory medicine.

This study has several limitations. First, its single-centre, retrospective design may introduce selection bias; multi-centre prospective cohorts are required for external validation. Second, prediction of FEV_1 %pred and FVC %pred lagged behind the remaining three spirometric indices, probably because the generic reference equations are not well calibrated to our population; future work should derive ethnicity-specific norms. Third, the under-representation of PRISm subjects produced class imbalance that biased the multiclass classifier; larger, balanced datasets are needed to confirm model performance. Finally, patients with concomitant significant lung disease were not excluded, limiting generalisability; subsequent studies should expand the spectrum of included pathologies to enhance robustness across heterogeneous populations. PRISm is attracting increasing attention, yet its recognition on chest CT remains challenging because of atypical imaging features and high inter-patient heterogeneity. Future models that add clinical data such as haematological and microbial biomarkers may speed progress in this area. Integrating diverse AI models such as omics or machine learning could further boost performance, and incorporating multitask learning may also be beneficial. Early detection of at risk individuals will allow prompt intervention, reduce disease burden and support the advance of precision medicine.

Conclusion

Self-attention-driven deep learning offers a powerful and scalable framework for chronic respiratory disease taxonomy and is poised to become a high-efficiency, clinician-friendly decision tool. The central contribution of this work is the inaugural demonstration that multimodal fusion of imaging and clinical data simultaneously enables robust classification of COPD, PRISm and normal together with accurate estimation of spirometric impairment, thereby establishing a methodological benchmark for future investigations. Subsequent studies will dissect how the learnt cross-modal representations correlate with histopathological severity, longitudinal disease progression and hard clinical outcomes, paving the way for precision-medicine algorithms that couple early phenotyping with individualized prognostication and therapy selection.

Patient and Public Involvement Statement

Patients or the public WERE NOT involved in the design, or conduct, or reporting, or dissemination plans of our research.

Patient Data Confidentiality Statement

Patient confidentiality is strictly maintained throughout this process. All medical records and personal information are handled in full compliance with HIPAA guidelines and institutional data protection protocols, accessible only to authorized research personnel through encrypted systems.

Abbreviations

COPD, Chronic obstructive pulmonary disease; PRISm, Preserved ratio impaired spirometry; PFT, Pulmonary function test; DL, Deep learning; CT, Computed tomography; FEV_1, 1-s Forced expiratory volume; FVC, Forced vital capacity; FEV_1/FVC, 1-s Forced expiratory volume ratio forced vital capacity; FEV_1 %pred, 1-s Forced expiratory volume to predicted value; FVC %pred, Forced vital capacity to predicted value; Grad-CAM, Gradient-weighted class activation mapping; GOLD, Global initiative for chronic obstructive lung disease; AUC, Area under the receiver-operating-characteristic curve; MSE, Mean-squared error; MAE, Mean absolute error; CCC, Concordance correlation coefficient.

Data Sharing Statement

The data that support the findings of this study are available from the corresponding author, upon reasonable request.

Ethics Approval and Consent to Participate

This study was conducted in accordance with the Declaration of Helsinki. Ethical approval was obtained from the Ethics Committee of the Fourth Clinical Medical College of Xinjiang Medical University, Urumqi, China (Approval 2025XE0165). As it did not involve the collection or disclosure of any personally identifiable information, the requirement for informed consent was waived by our ethic committee.

Author Contributions

All authors made a significant contribution to the work reported, whether that is in the conception, study design, execution, acquisition of data, analysis and interpretation, or in all these areas; took part in drafting, revising or critically reviewing the article; gave final approval of the version to be published; have agreed on the journal to which the article has been submitted; and agree to be accountable for all aspects of the work.

Funding

This study was supported in part by grants HXBYJSYS2024005 from Xinjiang Key Laboratory of Respiratory Disease Research.

Disclosure

The authors declare no competing interests in this work.

References

1. Mannino DM, Roberts MH, Mapel DW, et al. National and local direct medical cost burden of COPD in the United States From 2016 to 2019 and projections through 2029. *Chest*. 2024;165(5):1093–1106. doi:10.1016/j.chest.2023.11.040
2. Amegadzie JE, Mehareen J, Khakban A, Joshi P, Carlsten C, Sadatsafavi M. 20-year trends in excess costs of COPD. *Eur Respir J*. 2025;65(1). doi:10.1183/13993003.00516-2024
3. Wan ES, Fortis S, Regan EA, et al. Longitudinal phenotypes and mortality in preserved ratio impaired spirometry in the COPDGene Study. *Am J Respir Crit Care Med*. 2018;1(11):1397–1405. doi:10.1164/rccm.201804-0663oc
4. Kogo M, Sato S, Muro S, et al. Longitudinal changes and association of respiratory symptoms with preserved ratio impaired spirometry (PRISm): the Nagahama study. *Ann Am Thorac Soc*. 2023;20(11):1578–1586. doi:10.1513/annalsats.202301-050oc
5. Schwartz A, Arnold N, Skinner B, et al. Preserved ratio impaired spirometry in a spirometry database. *Respir Care*. 2021;66(1):58–65. doi:10.4187/respcare.07712
6. Wan ES, Castaldi PJ, Cho MH, et al. Epidemiology, genetics, and subtyping of preserved ratio impaired spirometry (PRISm) in COPDGene. *Respir Res*. 2014;15(1):89. doi:10.1186/s12931-014-0089-y
7. Wan ES, Hokanson JE, Regan EA, et al. Significant spirometric transitions and preserved ratio impaired spirometry among ever smokers. *Chest*. 2022;161(3):651–661. doi:10.1016/j.chest.2021.09.021
8. Ogata H, Sha K, Kotetsu Y, et al. The prognostic performance of lung diffusing capacity in preserved ratio impaired spirometry: an observational cohort. *Int J Chronic Obstr*. 2022;17:2791–2799. doi:10.2147/COPD.S384074
9. Shin YY, Park S, Kim KJ, et al. Clinical characteristics and medical utilization of smokers with preserved ratio impaired spirometry. *Int J Chronic Obstr*. 2023;18:2187–2194. doi:10.2147/COPD.S425934
10. Chen D, Curtis JL, Chen Y. Twenty years of changes in the definition of early chronic obstructive pulmonary disease. *Chin Med J Pulm Crit Care Med*. 2023;1(2):84–93. doi:10.1016/j.pccm.2023.03.004
11. Jo YS, Rhee CK, Kim SH, Lee H, Choi JY. Spirometric transition of at risk individuals and risks for progression to chronic obstructive pulmonary disease in general population. *Arch Bronconeumol*. 2024;60(10):634–642. doi:10.1016/j.arbres.2024.05.033

12. Kanetake R, Takamatsu K, Park K, Yokoyama A. Prevalence and risk factors for COPD in subjects with preserved ratio impaired spirometry. *Respir Res*. 2022;9(1). doi:10.2147/COPD.S384074
13. Agusti A, Hughes R, Rapsomaki E, et al. The many faces of COPD in real life: a longitudinal analysis of the NOVELTY cohort. *ERJ Open Res*. 2024;10(1). doi:10.1183/23120541.00895-2023
14. Martinelli M, Ponte EV, Pereira DAS, et al. Relationship between symptoms and results on spirometry in adults seen in non-tertiary public health facilities presenting with preserved ratio impaired spirometry. *Monaldi Arch Chest Dis*. 2024. doi:10.4081/monaldi.2024.2990
15. Liwsrisakun C, Chaiwong W, Deesomchok A, Duangjit P, Pothirat C. The role of impulse oscillometry in detection of preserved ratio impaired spirometry (PRISm). *Adv Respir Med*. 2025;93(1):2. doi:10.3390/arm93010002
16. Kang Z, Zhang J, Zhu C, et al. Impaired pulmonary function increases the risk of gout: evidence from a large cohort study in the UK Biobank. *BMC Med*. 2024;22(1):606. doi:10.1186/s12916-024-03836-8
17. Young KA, Regan EA, Han MK, et al. Subtypes of COPD have unique distributions and differential risk of mortality. *COPD*. 2019;6(5):400–413. doi:10.15326/jcopdf.6.5.2019.0150
18. Habteslassie D, Khorramnia S, Muruganandan S, et al. Missed diagnosis or misdiagnosis: how often do hospitalised patients with a diagnosis of chronic obstructive pulmonary disease have spirometry that supports the diagnosis? *J Intern Med*. 2023;53(4):510–516. doi:10.1111/imj.15607
19. Kim SH, Han MK. Challenges and the future of pulmonary function testing in Chronic Obstructive Pulmonary Disease (COPD): toward earlier diagnosis of COPD. *Tuberc Respir Dis*. 2025;88(3):413–418. doi:10.4046/trd.2025.0009
20. Dournes G, Zysman M, Benlala I, et al. CT imaging of chronic obstructive pulmonary disease: what aspects and what role? *Rev Mal Respir*. 2024;41(10):738–750. doi:10.1016/j.rmr.2024.10.002
21. Kinney GL, Young KA, Sansone-Poe DM, Alvarez MCP, Hokanson JE, Austin E. The correlational structure of lung CT and PFT in COPD are stable over five years. *Am J Respir Crit Care Med*. 2025;211:a1241. doi:10.1164/ajrccm.2025.211.abstracts.a1241
22. Exarchos K, Aggelopoulou A, Oikonomou A, et al. Review of artificial intelligence techniques in chronic obstructive lung disease. *Ieee J Biomed Health*. 2022;26(5):2331–2338. doi:10.1109/jbhi.2021.3135838
23. Robertson NM, Centner CS, Siddharthan T. Integrating artificial intelligence in the diagnosis of COPD globally: a forward. *COPD*. 2024;11 (1):114–120. doi:10.15326/jcopdf.2023.0449
24. Mostafa FA, Elrefaei LA, Fouda MM, et al. A survey on AI techniques for thoracic diseases diagnosis using medical images. *Diagnostics*. 2022;12 (12):3034. doi:10.3390/diagnostics12123034
25. Bian HP, Zhu SQ, Zhang YH, et al. Artificial intelligence in chronic obstructive pulmonary disease: research status, trends, and future directions -a bibliometric analysis from 2009 to 2023. *Int J Chronic Obstr*. 2024;19:1849–1864. doi:10.2147/COPD.S474402
26. Fernández AD, Fernández DR, Iglesias VG, et al. Analyzing the use of artificial intelligence for the management of chronic obstructive pulmonary disease (COPD). *Int J Med Inform*. 2022;158:104640. doi:10.1016/j.ijmedinf.2021.104640
27. Awan H, Chaudhary M, Gerard SE, et al. Deep residual convolutional network predicts future severe exacerbations of COPD in SPIROMICS. *Am J Respir Crit Care Med*. 2023;207:a3318. doi:10.1164/ajrccm-conference.2023.207.1_meetingabstracts.a3318
28. Zhou T, Guan Y, Lin X, et al. CT-based whole lung radiomics nomogram for identification of PRISm from non-COPD subjects. *Respir Res*. 2024;25(1):329. doi:10.1186/s12931-024-02964-2
29. Zhou T, Guan Y, Lin X, et al. A clinical-radiomics nomogram based on automated segmentation of chest CT to discriminate PRISm and COPD patients. *Eur J Radiol Open*. 2024;13:100580. doi:10.1016/j.ejro.2024.100580
30. Lukhumaidze L, Hogg JC, Bourbeau J, Tan WC, Kirby M. Quantitative CT imaging features associated with stable PRISm using machine learning. *Acad Radiol*. 2025;32(1):543–555. doi:10.1016/j.acra.2024.08.030
31. Ratiu IA, Ligor T, Bocos-Bintintan V, Mayhew CA, Buszewski B. Volatile organic compounds in exhaled breath as fingerprints of lung cancer, asthma and COPD. *J Clin Med*. 2020;10(1):32. doi:10.3390/jcm10010032
32. Saha PK, Nadeem SA, Comellas AP. A survey on artificial intelligence in pulmonary imaging. *Wiley Interdiscip Rev Data Min Knowl Discov*. 2023;13(6):e1510. doi:10.1002/widm.1510
33. Estepar RSJ. Artificial intelligence in COPD: new venues to study a complex disease. *Barc Respir Netw Rev*. 2020;6(2):144–160. doi:10.23866/brnrev:2019-0014
34. Chandrasekar V, Singh AV, Maharjan RS, et al. Perspectives on the technological aspects and biomedical applications of virus-like particles/nanoparticles in reproductive biology: insights on the medicinal and toxicological outlook. *Adva NanoBiomed Res*. 2022;2(8):2200010. doi:10.1002/anbr.202200010
35. Jesus FR, Moraes ACS, da Silva ILN, et al. Analysis of endocrine and inflammatory markers in preserved ratio impaired spirometry. *Med Sci*. 2024;12(2):18. doi:10.3390/medsci12020018
36. Cortes-Ibanez FO, Johnson T, Mascalchi M, Katzke V, Delorme S, Kaaks R. Serum-based biomarkers associated with lung cancer risk and cause-specific mortality in the German randomized Lung Cancer Screening Intervention (LUSI) trial. *Transl Lung Cancer Res*. 2023;12(12):2460. doi:10.21037/tlcr-23-548
37. Wu Q, Guo H, Li R, Han J. Deep learning and machine learning in CT-based COPD diagnosis: systematic review and meta-analysis. *Int J Med Inform*. 2025;196:105812. doi:10.1016/j.ijmedinf.2025.105812
38. Xu ST, Deo R, Soar J, et al. Automated detection of airflow obstructive diseases: a systematic review of the last decade (2013–2022). *Comput Meth Prog Bio*. 2023;241:107746. doi:10.1016/j.cmpb.2023.107746
39. Wu YN, Xia SY, Liang ZY, et al. Artificial intelligence in COPD CT images: identification, staging, and quantitation. *Respir Res*. 2024;25(1):319. doi:10.1186/s12931-024-02913-z
40. Von GT, Ghoreishi N, Björklund M, et al. Exponential growth of systematic reviews assessing artificial intelligence studies in medicine: challenges and opportunities. *Syst Rev*. 2022;11(1):132. doi:10.1186/s13643-022-01984-7
41. Li RY, Yang YH, Wu SL, et al. Using artificial intelligence to improve medical services in China. *Ann Transl Med*. 2020;8(11):711. doi:10.21037/atm.2019.11.108
42. Zou XL, Ren Y, Yang HL, et al. Screening and staging of chronic obstructive pulmonary disease with deep learning based on chest X-ray images and clinical parameters. *Bmc Pulm Med*. 2024;24(1):153. doi:10.1186/s12890-024-02945-7
43. Mehrotra R, Agrawal R, Ansari MA. Diagnosis of hypercritical chronic pulmonary disorders using dense convolutional network through chest radiography. *Multimed Tools Appl*. 2022;81(6):7625–7649. doi:10.1007/s11042-021-11748-5

44. Schiebler ML, Fain S. Hyperpolarized Noble Gas Ventilation MRI in COPD. *Radiology*. 2020;297(1):211–213. doi:10.1148/radiol.2020202855
45. Pippard BJ, Neal MA, Holland CW, et al. Assessing lung ventilation and bronchodilator response in asthma and chronic obstructive pulmonary disease with 19F MRI. *Radiology*. 2024;313(3):e240949. doi:10.1148/radiol.240949